4-25-2011

Effects of particle aggregation and disaggregation on their inherent optical properties

Wayne H. Slade
University of Maine

Emmanuel Boss
University of Maine, emmanuel.boss@maine.edu

Clementina Russo
University of Maine

Effects of particle aggregation and disaggregation on their inherent optical properties

Wayne H. Slade,[1,*] Emmanuel Boss,[1] and Clementina Russo[2]

[1]School of Marine Sciences, University of Maine, 360 Aubert Hall, Orono, ME 04469, USA
[2]*Department of Physics and Astronomy, University of Maine, 120 Bennett Hall, Orono, ME 04469, USA*
[*]*wayne.slade@gmail.com*

Abstract: In many environments a large portion of particulate material is contained in aggregated particles; however, there is no validated framework to describe how aggregates in the ocean scatter light. Here we present the results of two experiments aiming to expose the role that aggregation plays in determining particle light scattering properties, especially in sediment-dominated coastal waters. First, *in situ* measurements of particle size distribution (PSD) and beam-attenuation were made with two laser particle sizing instruments (one equipped with a pump to subject the sample to aggregate-breaking shear), and measurements from the two treatments were compared. Second, clays were aggregated in the laboratory using salt, and observed over time by multiple instruments in order to examine the effects of aggregation and settling on spectral beam-attenuation and backscattering. Results indicate: (1) mass normalized attenuation and backscattering are only weakly sensitive to size changes due to aggregation in contrast to theory based on solid particles, (2) the spectral slope of beam-attenuation is indicative of changes in PSD but is complicated by instrument acceptance angle, and (3) the spectral shape of backscattering did not provide as clear a relationship with PSD as spectral beam attenuation, as is predicted by theory for solid spheres.

OCIS codes: (010.4450) Oceanic optics; (010.4458) Oceanic scattering; (120.5820) Scattering measurements; (290.2200) Extinction; (010.1350) Backscattering; (290.5850) Scattering, particles.

References and links

1. D. Eisma, "Flocculation and de-flocculation of suspended matter in estuaries," Neth. J. Sea Res. **20**(2-3), 183–199 (1986).
2. I. McCave, "Particle size spectra, behavior, and origin of nepheloid layers over the Nova Scotian continental rise," J. Geophys. Res. **88**(C12), 7647–7666 (1983).
3. P. S. Hill, and A. R. M. Nowell, "Comparison of two models of aggregation in continental-shelf bottom boundary layers," J. Geophys. Res. **100**(C11), 22,749–22,763 (1995).
4. A. B. Burd, and G. A. Jackson, "Particle aggregation," Ann. Rev. Mar. Scie. **1**(1), 65–90 (2009).
5. I. G. Droppo, "Rethinking what constitutes suspended sediment," Hydrol. Process. **15**(9), 1551–1564 (2001).
6. W. R. Clavano, E. Boss, and L. Karp-Boss, "Inherent optical properties of non-spherical marine-like particles—from theory to observations," Oceanogr. Mar. Biol. **45**, 1–38 (2007).
7. C. Sorensen, "Light scattering by fractal aggregates: a review," Aerosol Sci. Technol. **35**, 648–687 (2001).
8. Y. Xu, and B. Gustafson, "Light scattering by an ensemble of small particles," Recent Res. Dev. Opt. **3**, 599–648 (2003).
9. P. Latimer, and F. Wamble, "Light scattering by aggregates of large colloidal particles," Appl. Opt. **21**(13), 2447–2455 (1982).
10. P. Latimer, "Experimental tests of a theoretical method for predicting light scattering by aggregates," Appl. Opt. **24**(19), 3231–3239 (1985).
11. K. L. Carder, and D. K. Costello, "Optical effects of large particles," in *Ocean Optics*, R. Spinrad, K. Carder, and M. J. Perry, eds. (Oxford university Press, 1994).
12. D. K. Costello, K. L. Carder, and W. Hou, "Aggregation of diatom bloom in a mesocosm: Bulk and individual particle optical measurements," Deep Sea Res. Part II Top. Stud. Oceanogr. **42**(1), 29–45 (1995).

#141939 - $15.00 USD Received 28 Jan 2011; revised 22 Mar 2011; accepted 31 Mar 2011; published 11 Apr 2011

13. W. Hou, K. L. Carder, and D. K. Costello, "Scattering phase function of very large particles in the ocean," Proc. SPIE **2963** (Ocean Optics XIII), 579–584 (1997).
14. A. Hatcher, P. Hill, and J. Grant, "Optical backscatter of marine flocs," J. Sea Res. **46**(1), 1–12 (2001).
15. E. N. Flory, P. S. Hill, T. G. Milligan, and J. Grant, "The relationship between floc area and backscatter during a spring phytoplankton bloom," Deep Sea Res. Part I Oceanogr. Res. Pap. **51**(2), 213–223 (2004).
16. E. Boss, W. H. Slade, and P. Hill, "Effect of particulate aggregation in aquatic environments on the beam attenuation and its utility as a proxy for particulate mass," Opt. Express **17**(11), 9408–9420, 420 (2009).
17. P. S. Hill, E. Boss, J. P. Newgard, B. A. Law, and T. G. Milligan, "Observations of the sensitivity of beam attenuation to particle size in a coastal bottom boundary layer," J. Geophys. Res. **116**(C2), C02023 (2011), doi:10.1029/2010JC006539.
18. E. Boss, W. S. Pegau, W. D. Gardner, J. R. V. Zaneveld, A. H. Barnard, M. S. Twardowski, G. C. Chang, and T. D. Dickey, "Spectral particulate attenuation and particle size distribution in the bottom boundary layer of a continental shelf," J. Geophys. Res. **106**(C5), 9509–9516 (2001).
19. S. Ackleson, "Optical determinations of suspended sediment dynamics in western Long Island Sound and the Connecticut River plume," J. Geophys. Res. **111**(C7), C07009 (2006), doi:10.1029/2005JC003214.
20. Y. C. Agrawal, and H. C. Pottsmith, "Instruments for particle size and settling velocity observations in sediment transport," Mar. Geol. **168**(1-4), 89–114 (2000).
21. M. S. Twardowski, J. M. Sullivan, P. L. Donaghay, and J. R. V. Zaneveld, "Microscale quantification of the absorption by dissolved and particulate material in coastal waters with an ac-9," J. Atmos. Ocean. Technol. **16**(6), 691–707 (1999).
22. WET Labs, Inc., "ECO Triplet User's Guide (triplet)," Revision P, 19 Jan. 2010. http://www.wetlabs.com/products/pub/eco/tripletp.pdf
23. W. H. Slade, and E. S. Boss, "Calibrated near-forward volume scattering function obtained from the LISST particle sizer," Opt. Express **14**(8), 3602–3615 (2006).
24. Y. C. Agrawal, A. Whitmire, O. A. Mikkelsen, and H. C. Pottsmith, "Light scattering by random shaped particles and consequences on measuring suspended sediments by laser diffraction," J. Geophys. Res. **113**(C4), C04023 (2008), doi:10.1029/2007JC004403.
25. Y. C. Agrawal, and O. A. Mikkelsen, "Empirical forward scattering phase functions from 0.08 to 16 deg. for randomly shaped terrigenous 1-21 microm sediment grains," Opt. Express **17**(11), 8805–8814 (2009).
26. E. Boss, M. S. Twardowski, and S. Herring, "Shape of the particulate beam attenuation spectrum and its inversion to obtain the shape of the particulate size distribution," Appl. Opt. **40**(27), 4885–4893 (2001).
27. M. S. Twardowski, H. Claustre, S. A. Freeman, D. Stramski, and Y. Huot, "Optical backscattering properties of the 'clearest' natural waters," Biogeoscie. **4**(6), 1041–1058 (2007).
28. G. Dall'Olmo, T. K. Westberry, M. J. Behrenfeld, E. Boss, and W. H. Slade, "Significant contribution of large particles to optical backscattering in the open ocean," Biogeosci. **6**(6), 947–967 (2009).
29. E. Boss, W. S. Pegau, M. Lee, M. S. Twardowski, E. Shybanov, G. Korotaev, and F. Baratange, "Particulate backscattering ratio at LEO 15 and its use to study particles composition and distribution," J. Geophys. Res. **109**(C1), C01014 (2004), doi:10.1029/2002JC001514.
30. C. R. Russo, E. S. Boss, W. H. Slade, and J. Newgard, "An investigation of the acoustic backscatter response to suspensions of clay aggregates and natural sediments," Cont. Shelf Res. (submitted).
31. K. J. Voss, and R. W. Austin, "Beam-attenuation measurements error due to small-angle scattering acceptance," J. Atmos. Ocean. Technol. **10**(1), 113–121 (1993).
32. E. Boss, W. H. Slade, M. Behrenfeld, and G. Dall'Olmo, "Acceptance angle effects on the beam attenuation in the ocean," Opt. Express **17**(3), 1535–1550 (2009).
33. K. Kranck, "Experiments on the significance of flocculation in the settling of fine-grained sediment in still water," Can. J. Earth Sci. **17**, 1517–1526 (1980).
34. K. Kranck, and T. G. Milligan, "Grain size in oceanography," in *Theory, Methods and Applications of Particle Size Analysis*, J. P. M. Syvitski, ed. (Cambridge University Press, New York, 1991).
35. K. J. Curran, P. S. Hill, and T. G. Milligan, "The role of particle aggregation in size-dependent deposition of drill mud," Cont. Shelf Res. **22**(3), 405–416 (2002).
36. O. A. Mikkelsen, P. S. Hill, and T. G. Milligan, "Single-grain, microfloc and macrofloc volume variations observed with a LISST-100 and a digital floc camera," J. Sea Res. **55**(2), 87–102 (2006).
37. D. W. Townsend, M. D. Keller, M. E. Sieracki, and S. G. Ackleson, "Spring phytoplankton blooms in the absence of vertical water column stability," Nature **360**(6399), 59–62 (1992).
38. N. Briggs, "Analysis of optical spikes reveals dynamics of aggregates in the twilight zone," University of Maine M.S. Thesis (2010). http://www.library.umaine.edu/theses/pdf/BriggsN2010.pdf
39. K. S. Shifrin, *Physical Optics of Ocean Water* (American Institute of Physics, 1995).
40. A. Khelifa, and P. S. Hill, "Models for effective density and settling velocity of flocs," J. Hydraul. Res. **44**(3), 390–401 (2006).
41. F. Maggi, "Variable fractal dimension: A major control for floc structure and flocculation kinematics of suspended cohesive sediment," J. Geophys. Res. **112**(C7), C07012 (2007), doi:10.1029/2006JC003951.

1. Introduction

The scattering of light in aquatic environments is dominated by the effects of particulate material. The intensity and spectral characteristics of scattering depend strongly on the concentration, composition, and particle size distribution (PSD) of suspended matter. In many

#141939 - $15.00 USD Received 28 Jan 2011; revised 22 Mar 2011; accepted 31 Mar 2011; published 11 Apr 2011

environments a large portion of suspended particulate material is packaged as aggregated particles [1], and the overall characteristics of the particulate matter pool are a result of multiple processes including resuspension, aggregation, and disaggregation [e.g., 2,3]. Aggregation and disaggregation affect changes in particle porosity and size, and the composition of an aggregate is remarkably dynamic, reflective of the heterogeneity of its physical, biological, and chemical environments, as well as to its role as a scavenger, gaining and losing material as it is transported throughout the water column [e.g., 4,5]. Components of marine aggregates include bacteria, organic and inorganic colloids, algal particles and associated detritus, mineral particles, as well as polymers, fibrils, and gels, originating biologically and abiotically. Despite the profound consequences of aggregation, there is no accepted framework to describe the effects of aggregation on the scattering properties of suspended particulate material, and the idealized model of the homogenous sphere remains dominant in the study of particle optical properties [6]. However, consideration of particle packaging is likely needed for the extension of optical methods into environments such as river plumes, bottom boundary layers, and phytoplankton blooms.

The optical properties of aggregates have attracted substantial attention in disciplines other than oceanography, mostly relating to aerosols, interstellar dust, and colloids. Such studies are usually concerned with loose (diffusion limited) fractal aggregates constructed of submicron monomer particles smaller than the wavelength of incident light. Some of these algorithms invoke a (relatively) simple superposition of Rayleigh-Debye-Gans scattering for each monomer, ignoring internal scattering [e.g., 7], while others consider a rigorous Mie-based multiple scattering solution [e.g., 8]. Invariably, despite simplifying assumptions, these approaches are defeated by computational limitations for the particle sizes relevant to aquatic aggregates. In contrast, Latimer and Wamble [9] presented a model describing the scattering properties of aggregates whose component particles are somewhat larger than the wavelength of incident light. They hypothesize that light scattering due to a suspension of randomly-oriented aggregates caries only information about the overall size and porosity (void fraction) of the aggregates. Given this assumption, they then approximated the optical effects of aggregate structure on optical properties using models for randomly-oriented spheroids and coated spherical particles having equivalent gross volume and net mass as the aggregates. Results from their simple model and experimental data from suspensions of latex sphere aggregates agreed to first order, with some of the disagreement likely explained by inaccuracies inherent in the microscopic analysis of the aggregates [10].

There are few studies of the optical properties of marine aggregates in the laboratory or field. Early work by Carder and Costello [11] qualitatively considered the effects that aggregation could have on observational closure of optical properties by packaging mass into particles that are large and rare relative to the measurement sample volume. Costello et al. [12] examined variability of optical properties during a controlled diatom bloom mesocosm study and found beam-attenuation to be an excellent indicator of particulate organic carbon despite changes in PSD, and saw increase in the variance of optical properties as the diatom population aggregated. In a follow-up to their previous work, Hou et al. [13] later used a specialized instrument to measure the scattering properties and PSD of marine snow particles greater than 280 μm throughout the water column and concluded that these large particles could contribute up to 20% of total scattering as well as enhance backscattering efficiency. More recently, Hatcher et al. [14] examined the optical backscattering of phytoplankton-drill mud aggregates created in the laboratory using an upwelling tank. During the course of the 37-day experiment, during which the aggregates formed and aged, the relationship between backscattering and projected cross-sectional area for particles greater than 10 μm in diameter remained constant. A subsequent experiment by Flory et al. [15] observed backscattering and PSD (for particles greater than approximately 100 μm in diameter), and found evidence that the effect of large particles on backscattering has been underestimated. However, none of these studies independently measured particles less than 10 μm, which we would expect not only to be highly efficient scatterers, but also to be correlated with the concentration of aggregates because of the role of aggregates as particle scavengers.

#141939 - $15.00 USD Received 28 Jan 2011; revised 22 Mar 2011; accepted 31 Mar 2011; published 11 Apr 2011

The mass-specific optical properties of aggregates will differ from solid particles as a result of the fractal nature of an aggregate, where the large fluid fraction within the aggregate results in a cross-sectional area that is larger than that of a solid particle of the same mass. Previously [16], we examined the beam-attenuation of marine particles using Latimer's model [9,10] that approximates aggregate particle structure as an ensemble of hollow spheres and randomly-oriented ellipsoids, with aggregate porosity a function of size. Using a traditional homogenous sphere model, mass-specific beam-attenuation varied significantly as a function of changing PSD. However, with the aggregate model, we found mass-specific attenuation to be remarkably constant and consistent with observations of marine particles in the environment encompassing a wide range of particle sizes and composition [17].

Finally, two additional studies have considered potential effects of particle dynamic processes on bulk inherent optical properties. Boss et al. [18] examined the tight relationship between particulate beam-attenuation magnitude and spectral slope (an indicator of PSD slope), and found the two parameters to be consistent with resuspension and size-dependent settling in the bottom boundary layer for most of their data. Deviation from this tight relationship occurred on the sampling day following a passing hurricane, and the authors consider aggregation dynamics to be a possible explanation for their observations. More recently, Ackleson [19] used a simple model linking optical properties derived from Mie theory and changes in PSD expected from disaggregation and settling scenarios to examine Long Island Sound and Connecticut River plume data, finding that disaggregation was able to explain optical variability at the plume boundary. However, Ackelson also found that changes in spectral slope may also be explained by mixing between the two water masses, and concluded that the method of using spectral optical properties to examine particle dynamics requires additional research.

To further increase our understanding of the effects of particle aggregation on optical properties, we conducted an *in situ* manipulation experiment, measuring and comparing optical properties of the natural suspension and the natural suspension subjected to shear (in order to break aggregates). Using two Sequoia Scientific LISST-100 instruments (measuring near-forward scattering and beam-attenuation) [20], one open to the environment and the other employing a sample chamber and pump, this experiment allowed us to qualitatively examine the effect of aggregation on beam-attenuation.

A second experiment was conducted in the laboratory to further investigate the effects of packaging of particles into aggregates. In this experiment, clays were aggregated using salt and observed over time by a LISST-100X instrument, open-path WET Labs ac-9 [21] (measuring multi-spectral beam-attenuation), and a WET Labs ECO Triplet (measuring volume scattering function, VSF, at 117° at three wavelengths) [22], in order to examine the effects of increasing aggregate size on optical properties.

2. Experimental setup, procedures, and data processing

2.1 LISST PSD and beam-attenuation

The LISST-100 (Sequoia Scientific, Inc.) is an in-water instrument designed to measure PSD in the field. The LISST-100 infers PSD from the scattering of a red laser beam (670 nm) introduced into a sample volume (5-cm path-length). The beam is scattered by particulate material within the sample volume, and near-forward scattered light at angles ranging from approximately 0.075° to 14.9° is received by a Fourier lens and transformed onto a set of 32 logarithmically-spaced, co-planar, concentric photodetector rings. For large particles that scatter light more near-forward, the most inner of the concentric photodetectors respond. Conversely, as particle size increases, angular light scatter becomes less concentrated in the near-forward and response increases in photodetectors further from the center. In addition, photodetectors measure transmitted (0.0269° acceptance angle) and reference (beam-split) laser power in order to estimate beam-attenuation $c_{pg}(670)$, where "pg" refers to combined particulate and dissolved components. Before each field or laboratory experiment, blank measurements (*zscat*) were made with the manufacturer-supplied software using Barnstead

#141939 - $15.00 USD Received 28 Jan 2011; revised 22 Mar 2011; accepted 31 Mar 2011; published 11 Apr 2011

NANOpure water in the small volume chamber insert or by filling the laboratory sink with reverse osmosis (RO) water. In both cases the water was allowed to sit to reduce the effects of bubbles, and blank measurements were repeated (with instrument cleaning) until our *zscat* scattering patterns were comparable in shape but lower in amplitude than those supplied by the manufacturer. Raw scattering due to particulates could then be calculated by subtraction of the *zscat* from measurements made during the experiments [20,23]. Data processing and PSD inversion for the LISST was performed on un-binned data, and subsequently binned to five-minute intervals or burst-averaged.

Sequoia Scientific supplies an algorithm [20] to invert the angularly-resolved scattering pattern into a volume PSD ($V(D_i)$ in units of μL/L) having 32 size classes with geometric mean diameters (D_i, i={1, 2…32}) from approximately 1 μm to 184 μm. We used an updated version of the inversion kernel based on scattering by randomly-shaped natural particles [24,25]. In order to condense changes in PSD into a single parameter, we employ a weighted-average particle size calculated as

$$D_{avg} = \sum_{i=1}^{32} A(D_i) D_i \Big/ \sum_{i=1}^{32} A(D_i), \qquad (1)$$

where $A(D_i)$ is the areal PSD in suspended cross-sectional area per volume ($m^2\ m^{-3}$) for each LISST size class i, with mean diameter D_i. Areal size distribution (m^2/m^{-3}) is calculated from volume size distribution (μL/L) by assuming spherical geometry: $A(D_i) = \frac{3}{2} V(D_i) D_i^{-1}$.

2.2 ac-9 spectral attenuation measurements

The WET Labs, Inc. ac-9 [21] is a combination spectral beam transmissometer (0.93° acceptance angle) and reflecting-tube absorption meter, normally measuring absorption and beam-attenuation at nine illumination wavelengths in the visible spectrum (412–715 nm) by use of a rotating filter wheel in the light source. In the laboratory aggregation experiment we used a 10-cm path-length version and left the absorption tube sealed, but left the transmissometer-side open to the environment with no flow sleeve so that aggregates would fall through the illuminated sample volume undisturbed. The ac-9 was blanked in the laboratory sink using RO water, and particulate beam-attenuation was then calculated by difference of the experimental measurement and blank.

Particulate beam-attenuation spectra from the ac-9 were fit to a power-law function of the form $c_p(\lambda) = A\lambda^{-\gamma}$ by unconstrained nonlinear optimization (MATLAB "fminsearch") [18,26] using all available wavelengths except 715 nm. For ac-9 data from the laboratory experiment, the percent difference of the fit residuals relative to measured data was in general less than 2%.

2.3 ECO Triplet volume scattering function measurements

A WET Labs, Inc. ECO Triplet BB-3 was used to measure the VSF at a fixed angle of 117°, $\beta(117°, \lambda)$, at three wavelengths (λ = 532, 660, 880 nm), with a sampling rate of ~1 Hz. The BB-3 was calibrated at the factory with 2-μm polystyrene microspheres in order to determine a scaling factor and dark offset, S and D, respectively. The calibration values S and D are used to determine $\beta(117°, \lambda)$ from raw instrument digital counts, C, according to $\beta(117°, \lambda) = S(C - D)$ [22,27,28]; and particulate volume scattering is calculated by difference of the RO water blank, $\beta_{blank}(117°, \lambda)$, from measurements, $\beta_{tot}(117°, \lambda)$, made during the experiment:

$$\beta_p(117°, \lambda) = \beta_{tot}(117°, \lambda) - \beta_{blank}(117°, \lambda).$$

#141939 - $15.00 USD Received 28 Jan 2011; revised 22 Mar 2011; accepted 31 Mar 2011; published 11 Apr 2011

Thus the effects of the dark offset, D, were subtracted out. Path-length attenuation correction was not performed since absorption measurements were not available. For typical environmental measurements with absorption below 1 m□1, error is expected to be small, 4% [22,29]. Assuming a single scattering albedo for particles of ~0.95 and a maximum particulate attenuation of ~10 m□1, we expect our particulate absorption was less than 1 m□1, however this remains a potential error in our estimates of $\beta_p(117°,\lambda)$.

The spectral shape of un-binned $\beta_p(117°,\lambda)$ data was examined in a similar way as $c_p(\lambda)$. We found fits to the form $\beta_p(117°,\lambda) = A\lambda^{-\gamma_{bb}}$ to have percent differences of greater than 25%, with an obvious trend across the wavelength channels, indicating that a power-law fit is not suitable to our measurements. Therefore, ratios of individual wavelength pairs were also considered in order to reduce the possible influence of calibration (slopes, *S*) errors; the channel ratios were transformed to an equivalent γ_{bb},

$$\gamma_{bb}(\lambda_1,\lambda_2) = \log\left(\frac{\beta_p(\lambda_2)}{\beta_p(\lambda_1)}\right) \Big/ \log\left(\frac{\lambda_1}{\lambda_2}\right). \quad (2)$$

To help reduce noise in $\beta_p(117°,\lambda)$ data (likely due to separation of the sample volume of each wavelength channel), $\beta_p(117°,\lambda)$ was binned to 15-minute intervals for calculation of γ_{bb}.

2.4 In situ disaggregation experiment

The qualitative effect of aggregation on beam-attenuation was observed by comparing the measurements of two similar LISST-100 (Type B) instruments deployed side-by-side with one having a mechanism to break aggregates prior to the sample being measured. The instruments were deployed in the same package at ~1 m above bottom in the Damariscotta River Estuary (~10 m mean water depth), Walpole, ME over approximately 24 hours. The first of the instruments (LISST A) was open to the environment while the second (LISST B) sampled water that was introduced to a sampling chamber via a pump (SeaBird SBE 5T, 3000 rpm) intended to break aggregates through increased turbulent shear, denoted by the superscripts "(open)" and "(shear)," respectively. Note that the shear is not quantified, nor do we know what percent of aggregates were broken; thus the comparison of measurements between the two treatments provides only a qualitative indication of the effect aggregation has on the optical properties as measured by the LISST. During the last two hours of the deployment, the sample chamber and pump were removed from the second instrument so that both instrument sample volumes were open to the environment. Both instruments were configured to sample in bursts, timed at five minute intervals. LISST measurements were processed using standard methods and then burst-averaged.

2.5 Laboratory aggregation experiment

The laboratory experiment was performed in order to examine how aggregation affects optical properties as a function of increasing aggregate size. Two beam transmissometers (a LISST–100 Type B, acceptance angle 0.0269° and an ac-9, acceptance angle 0.93°) were arranged side by side with their sampling volumes open to the environment in the bottom of a large 100×40×45-cm sink. The LISST measured both beam-attenuation and near forward scattering, which was inverted to PSD as described earlier. While both sample volumes were open to allow aggregates to sink through them, we assume the contribution of dissolved materials that might be released by the clay to be negligible during the experiment and refer to attenuation as c_p rather than c_{pg}. A WET Labs ECO-BB3 was used to measure backscattering at a single angle in the backwards direction, at three illumination wavelengths (532, 660, 880 nm). Care was taken to position all instruments to sample at the same depth.

#141939 - $15.00 USD Received 28 Jan 2011; revised 22 Mar 2011; accepted 31 Mar 2011; published 11 Apr 2011

The tank was also outfitted with sampling tubes having inlets at the instrument sampling depth. Samples (100 mL, in triplicate) were pumped gently at regular intervals throughout the experiment. Suspended particulate mass measurements (SPM) were made gravimetrically, using dried and pre-weighed 0.8-μm polycarbonate filter pads, and included a 100-mL deionized water rinse to remove accumulated salts. All data were captured by a single PC during the experiment, and later processed (time-stamping, calibration, inversion, and time-binning) in MATLAB. Calibration, correction, and data processing were performed using standard methods, and subsequently measurements were time-binned to five-minute intervals. D_{avg} was calculated according to Eq. (1) for the individual LISST measurements within each time bin.

On the day of the experiment, the sink and all instruments were first cleaned thoroughly. The sink was then filled with particle-free reverse-osmosis water, which was allowed to degas and was used to blank all instruments in the sink. A slurry of bentonite clay was disaggregated by vigorous stirring for ~30 minutes and then added and mixed into the water (4 g dry weight in 120 L of water, producing an environmentally relevant mass concentration of approximately 33 g m^{-3}). A calcium chloride solution (0.4 g CaCl L^{-1}) was then mixed into the sink to initiate particle aggregation. Note that this procedure was repeated with differing instrumentation before the specific experiment discussed here, and in each case results were very similar, differing slightly in the timing of aggregation and sinking. Sampling protocol for the SPM measurements are described in more detail in Russo et al. [30].

Mass-specific optical properties ($c^*_{p,LISST}$, $c^*_{p,ac9}$, β^*_p) are calculated using the binned data nearest the SPM measurements *M*, for example $\overline{c}^*_p = \overline{c}_p \big/ \overline{M}$, where bar notation indicates bin or triplicate mean value. Uncertainty in the mass-specific optical properties is determined by standard propagation of uncertainty, for example,

$$\delta c^*_p = \overline{c}^*_p \left(\left(\frac{\delta M}{\overline{M}} \right)^2 + \left(\frac{\delta c_p}{\overline{c}_p} \right)^2 \right)^{1/2}, \tag{3}$$

where δ denotes standard deviation of the triplicate or binned measurements.

3. Results and discussion

3.1 In situ disaggregation experiment

PSD inverted from the LISST scattering measurements reveal disappearance (destruction) of large particles by the pump and creation of smaller particles consistent with disaggregation (Fig. 1A). During the control period, the size spectra for the two different instruments were very similar in shape (Fig. 1B). A time series of attenuation and D_{avg} during the experiment (Fig. 2A,B) shows strong semi-diurnal tidal variability. Beam-attenuation for the open treatment $c^{(open)}_{pg}$ exhibits 12-hour variability suggesting that overall concentration at the site is advection-dominated; $c^{(open)}_{pg}$ minima correspond to high tide and $c^{(open)}_{pg}$ maxima to low tide where stronger riverine input to the partially-mixed estuary is expected. Both the attenuation ratio $c^{(shear)}_{pg} \big/ c^{(open)}_{pg}$ and open treatment $D^{(open)}_{avg}$ exhibit peaks every six hours when tidal currents (and consequently bottom stress and in-water shear) are strongest. This variability in $D^{(open)}_{avg}$ suggests physical control on aggregate size, while $D^{(shear)}_{avg}$ exhibits less variability during the experiment, suggesting that the PSD of the disaggregated population is more constant.

#141939 - $15.00 USD Received 28 Jan 2011; revised 22 Mar 2011; accepted 31 Mar 2011; published 11 Apr 2011

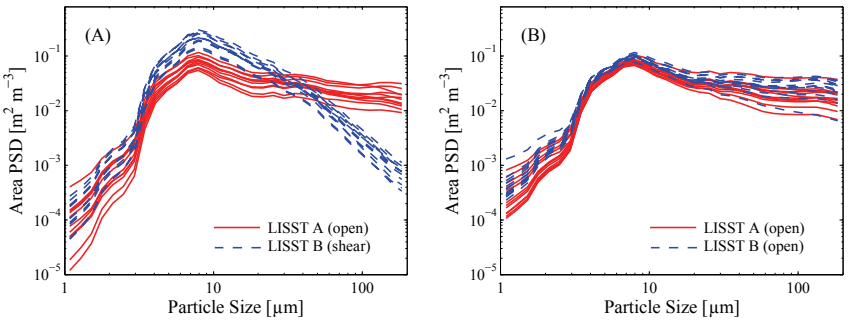

Fig. 1. – PSD for the two treatments: (A) during the experiment when LISST B was fitted with a sample chamber fed by a pump to subject aggregates to shear, and (B) during the control when both LISST sample volumes were open to the environment.

The beam-attenuation in the sheared treatment is ~30% higher (relative to control) compared to the open treatment (Fig. 2C), consistent with the idea that the smaller particles are more efficient attenuators per mass, though significantly less so than predicted by theory of solid particles [16]. These results also suggest that a large fraction of the particles contributing to the beam-attenuation are aggregates and that aggregation and disaggregation affect the beam-attenuation measured with the LISST. The observed effects on the beam-attenuation (as opposed to PSD inversion) are due either directly from changes in attenuation efficiency between the two treatments, or indirectly by making less material scatter within the acceptance angle of the instruments [31,32]. For the latter to be important, particles greater than ~400 µm would have to be broken, based on the acceptance angle of the LISST [32].

3.2 Laboratory aggregation experiment

PSD derived from the LISST (Fig. 3A) show a suspension initially dominated by small particles (~5 µm, likely tightly-bound clay micro-aggregates). Formation of a population of aggregates is clear in the PSD, as it grows in both modal size and magnitude (first clearly visible as a bump at ~60 µm). The mode of the aggregate population grows and eventually appears to exceed the maximum size bin of our LISST instrument (large "snowy" aggregates were clearly visible to the naked eye after ~2 h). As particles aggregated in our tank, the effects of settling and scavenging eventually began to dominate: large aggregates settle out of suspension, and through their large capture cross-section, scavenge and incorporate smaller particles [e.g., 33–35]. The final (red wide-dashed) PSD shows a significant and unbiased decrease in fine particles less than ~20 µm, expected as a result of scavenging by the large settling aggregates. In a previous experiment (identical setup, but with different instrumentation), we examined samples from the start of the experiment and ~1.5 h later with a microscope equipped with digital camera (Fig. 4). The microphotographs provide additional confidence in the LISST measurements, as the initial population (Fig. 4A) appears to be single particles, and aggregates are clearly visible in the image from ~1.5 h (Fig. 4B). Furthermore, the size of aggregates in Fig. 4B (approximately 75–100 µm) agrees roughly with the modal diameter of the aggregate population seen at ~1.5 h in Fig. 3A.

#141939 - $15.00 USD Received 28 Jan 2011; revised 22 Mar 2011; accepted 31 Mar 2011; published 11 Apr 2011

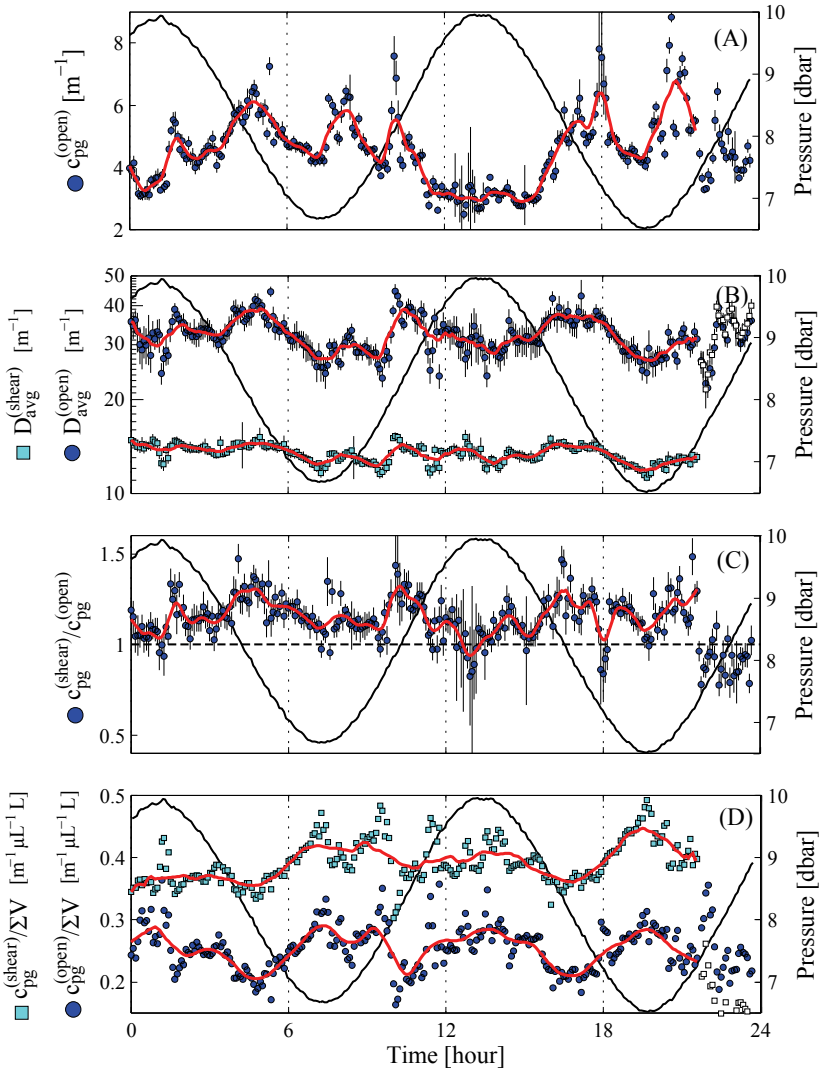

Fig. 2. – Time series of optical and particle size properties during the *in situ* disaggregation experiment. The experimental package was deployed in a bottom-mounted configuration thus tidal variability is shown as pressure in each plot. Unfilled symbols indicate the control data where the pump and sample chamber were removed from LISST B and both instruments were open to the environment. (A) Beam-attenuation for the open treatment. (B) Average particle size for both treatments. (C) The ratio of beam-attenuation from the two treatments. (D) The ratio of beam-attenuation to volume concentration as measured by the LISST, indicative of aggregates (see text).

The evolution of aggregation during the experiment can be illustrated by dividing the PSD into three distinct pools: (1) primary particles smaller than 6 μm, (2) small aggregates from 6 to 60 μm, and (3) large aggregates greater than 60 μm [36]. Area concentration in primary particles decreases throughout the experiment as they themselves form aggregates and/or are scavenged by larger aggregates settling. Initially, small aggregates are formed, leading to formation of larger aggregates, sweeping both primary particles and smaller aggregates from the water. The rate of decrease in primary particles is highest as large aggregates dominate, due to scavenging. Evolution of the area-weighted average size, D_{avg}, can also be seen in Fig.

#141939 - $15.00 USD Received 28 Jan 2011; revised 22 Mar 2011; accepted 31 Mar 2011; published 11 Apr 2011

3B and shows rapid aggregation (increase in D_{avg} until ~2 h after the start of the experiment), followed by settling and scavenging (slow reduction in D_{avg}).

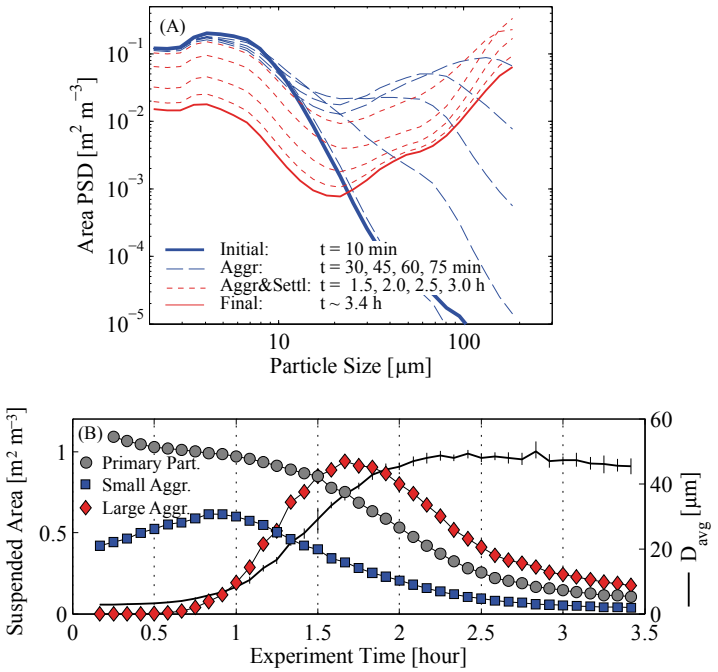

Fig. 3. – (A) LISST PSD snapshots over time. The thick blue line represents the distribution shortly (~10 min) after the start of the experiment, with the suspension dominated by small particles. Blue long-dashed PSD show the evolution of aggregated particles during the predominantly aggregation phase of the experiment. The red short-dashed lines show the evolution of PSD as settling and particle scavenging become more important. As a function of time, the population changes from domination by small particles to bi-modal. The thin red line shows the final measurement made by the LISST approximately 3.4 h after starting. (B) Time series of suspended area concentration for three size ranges of particles corresponding to primary particles, small aggregates, and large aggregates, as well as average particle size. Error bars for D_{avg} indicate 16th and 84th percentiles (the difference of which is twice the standard deviation in the case of a normal distribution) for binned data.

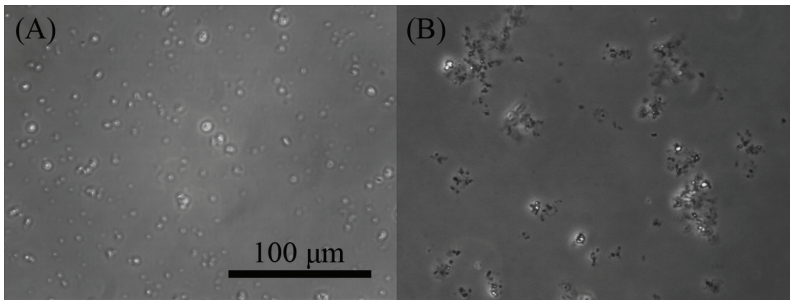

Fig. 4. – Microphotographs of the particle suspension made during a previous experiment with identical setup but different instrumentation. Initially, particles are disaggregated (A), but after ~1.5 h (B) aggregates are visible. Scale bar is for both (A) and (B). Note that particle size in (A) appears exaggerated due to halos.

#141939 - $15.00 USD Received 28 Jan 2011; revised 22 Mar 2011; accepted 31 Mar 2011; published 11 Apr 2011

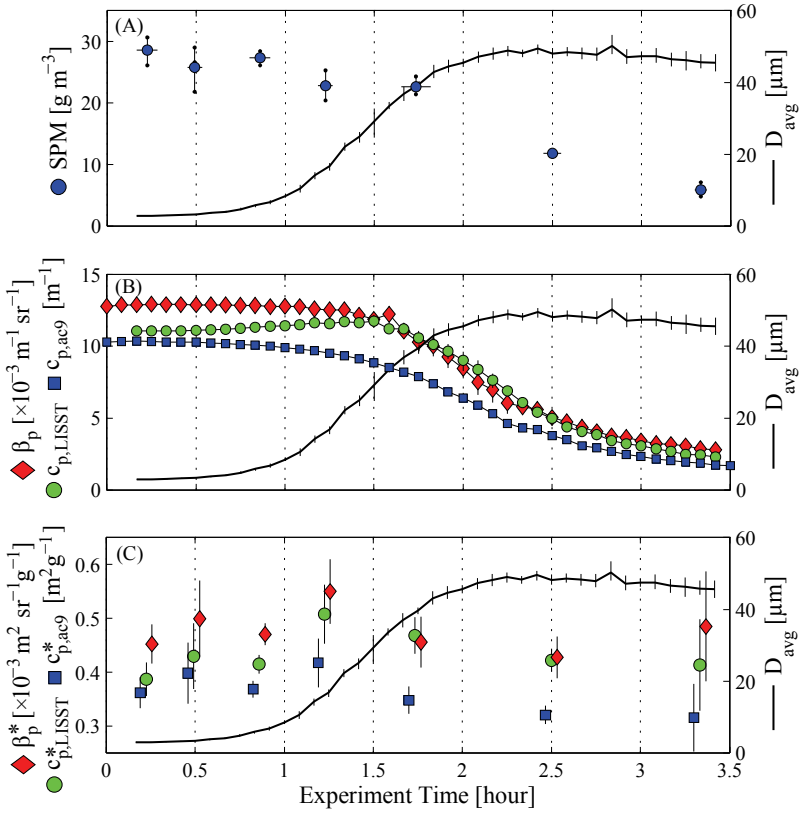

Fig. 5. – (A) Time series of average particle size, D_{avg}, calculated from area PSD measurements derived from the LISST during the laboratory aggregation-settling experiment, along with measurements of suspended particulate mass (SPM). For SPM, small black dots and the large blue dots represent the individual measurements and mean of triplicate measurements, respectively. Horizontal error bars show the duration of sampling. (B) Time series of beam-attenuation measured using the two transmissometers with different acceptance angles, as well as volume scattering function measured at 117° in the backwards direction. Each optical property shows decrease concurrent with decrease in suspended mass. (C) Mass-normalized optical properties are relatively constant despite changes in PSD during experiment. Uncertainty has been propagated according with standard methods, as Eq. (3). Note that symbols in (C) are offset slightly for clarity.

As particles aggregated and settled out of the water column (seen as a decrease in measured SPM, Fig. 5A), the values of the optical properties decreased rapidly (Fig. 5B). However, throughout the experiment, mass-specific c_p and β_p (c_p^* and β_p^*) remained remarkably constant (Fig. 5C) during changes in PSD (mean absolute deviations of 7.0%, 7.9%, and 6.1% relative to mean values of 0.43 m^2 g^{-1}, 0.36 m^2 g^{-1}, and 0.48 × 10^{-3} m^2 sr^{-1} g^{-1}, $c_{p,LISST}^*(670\text{nm})$, $c_{p,ac9}^*(660\text{nm})$, and $\beta_p^*(660\text{nm})$, respectively). Our proposed explanation for these observations is that aggregates are much more efficient scatterers per mass than Mie theory would suggest for solid particles of the same size, nearly conserving the cross-sectional area of their primary particles as they aggregate [16]. We also observed an increase in the variability of the measured optical properties (Fig. 5B) within each time bin as aggregates formed and settled through the sample volumes, causing spikes in raw measured data. Spikes in optical data have been previously linked to "rare large particles" and aggregation of phytoplankton following blooms [12,37,38]; and a method has been proposed to estimate particle size from fluctuations in beam-attenuation measurements [39].

#141939 - $15.00 USD Received 28 Jan 2011; revised 22 Mar 2011; accepted 31 Mar 2011; published 11 Apr 2011

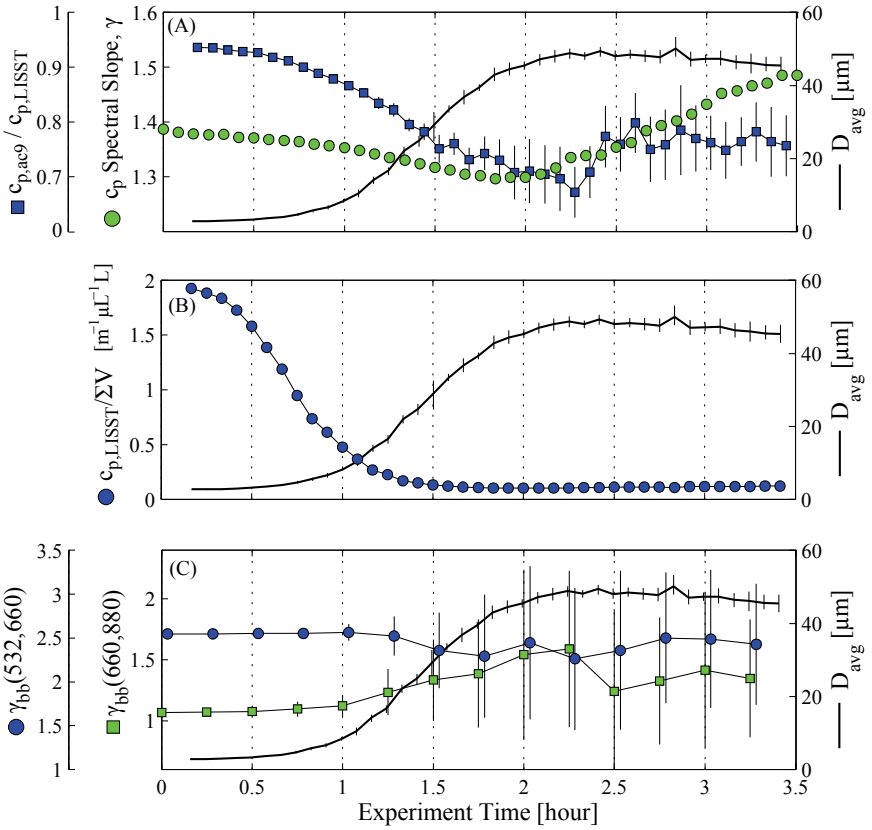

Fig. 6. – (A) Time series of beam-attenuation spectral slope and ratio of beam-attenuation for instruments (ac-9 and LISST) with differing acceptance angle. (B) The ratio of beam-attenuation to volume concentration as measured by the LISST, indicative of aggregate density. (C) Spectral shape of volume scattering function at 117° for two wavelength pairs (circles, squares) as well as the power law fit to all three wavelengths (diamonds). Note that symbols in (A) and (C) are offset slightly for clarity.

Deviation between beam-attenuation measured by the ac-9 and LISST is also evident in Fig. 6A. This deviation is consistent with differences in acceptance angles of the LISST and ac-9 since the larger acceptance angle of the ac-9 compared to the LISST collects more near-forward light scattered by large particles [31,32]. We find that the ratio of beam-attenuations from the two instruments correlates well with the average particle size (Fig. 7). This relationship is not due to the optical peculiarities of aggregates, but rather to the effects of particle size on near-forward scattering. Departure from the correlation for large D_{avg} is likely due to the presence of large aggregates beyond the size range resolved by the LISST inversion.

#141939 - $15.00 USD Received 28 Jan 2011; revised 22 Mar 2011; accepted 31 Mar 2011; published 11 Apr 2011

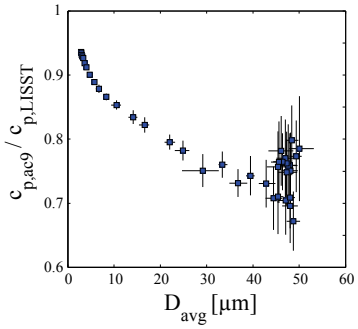

Fig. 7. – The ratio of beam-attenuations from instruments with different acceptance angle is strongly correlated with average particle size. As particle size increases, scattering is increased in the near-forward angles; resulting in a greater amount of light captured (transmitted rather than attenuated) by the wider acceptance angle of the ac-9.

3.3 Spectral optics, particle dynamics, and particle packaging

Observations and optical theory have shown that beam-attenuation spectra can be approximated well as a power law function of wavelength, $c_p(\lambda) = A\lambda^{-\gamma}$, and that the power-law exponent, γ, has further been shown be related to particle size [26]. It has been suggested that the relationship between the magnitude of $c_p(\lambda) = A\lambda^{-\gamma}$ and its slope γ is an indicator of particle dynamical processes [18,19]. For particle settling, a process highly dependent on size, we expect that beam-attenuation magnitude will decrease as mass settles out of suspension and its slope will steepen as larger particles settle faster than smaller particles. For aggregation, we expect that beam-attenuation magnitude will decrease as fine particles (more efficient scatterers per mass) are incorporated into aggregates, and that spectral slope will flatten as large particles are created from small particles. Figure 8A shows the progression of beam-attenuation versus spectral slope for the entire experiment. The aggregation-dominated portion of the experiment progresses along a course consistent with aggregation as beam-attenuation magnitude decreases and its slope flattens (decreases). As aggregation continues, increasing particle size to the point where settling dominates, the course is consistent with settling as beam-attenuation magnitude decreases and its slope steepens. Similar patterns have been observed in bottom boundary layers [18] and have been explained as being associated with aggregation and settling. Additionally, the acceptance angle of the ac-9 limits the contribution of larger particles to measured beam-attenuation, whereas the LISST and BB-3 sensors are more responsive to such particles. In fact, Fig. 8B shows the expected relationship between spectral slope, γ, and D_{avg} as particles aggregate over the first ~2 h of experiment, followed by a dramatic increase in γ (steepening) of the spectral shape. The increase in the latter part of the experiment is expected as aggregates grow to the point where they are no longer perceived by the ac-9 due to acceptance angle effects; and also because as the aggregates settle we expect them to leave a stranded population of fine particles.

The spectral shape of backscattering γ_{bb} (here in terms of VSF, $\beta_p(117°, \lambda)$) was also examined during the experiment (Fig. 6C), as there is expectation that it will be useable as an indicator of particle size similar to γ derived from beam-attenuation (for example, using small backscattering sensors easily incorporated into small autonomous platforms). As described in the methods section, a power law function was fit to measured data from the three wavelength channels (not shown). Spectral shape was also calculated using pairs of wavelengths and Eq. (2). In each case, the calculated $\gamma_{bb}(\lambda_1, \lambda_2)$ were very noisy in the presence of aggregates, making interpretation difficult. As particle size increased early during

#141939 - $15.00 USD Received 28 Jan 2011; revised 22 Mar 2011; accepted 31 Mar 2011; published 11 Apr 2011

aggregation, trends in $\gamma_{bb}(532,660)$ and $\gamma_{bb}(660,880)$ were apparent, but opposite, with $\gamma_{bb}(532,660)$ decreasing. The spectral slope expressed as $\gamma_{bb}(532,660)$ flattened as aggregates were formed, similar to γ from $c_p(\lambda)$, suggesting that information about particle size may be contained within spectral backscattering; however it is difficult to interpret the data after large aggregates dominate due to variability in the measurement due to spikes.

Finally, an additional diagnostic of particle packaging is the ratio of the beam-attenuation to total volume concentration (ΣV), as measured and inverted by the LISST. The beam-attenuation has been shown to be a reliable proxy for SPM [17], and assuming that the volume distribution from the LISST is reflective of the enclosing volume of aggregates, this ratio $c_{p,LISST}/\Sigma V$ is proportional to the density of the aggregate. In the field experiment, we find $c_{p,LISST}/\Sigma V$ for the open treatment to be lower than the shear treatment, suggesting the particles in the open treatment are less dense (Fig. 2D), and furthermore, the ratio exhibits a six-hour periodicity, as in $D_{avg}^{(open)}$, suggesting physical control on size and packaging. In the laboratory, $c_{p,LISST}/\Sigma V$ drops sharply as aggregate size increases, which is consistent with a decrease in aggregate density (Fig. 6B) [40,41].

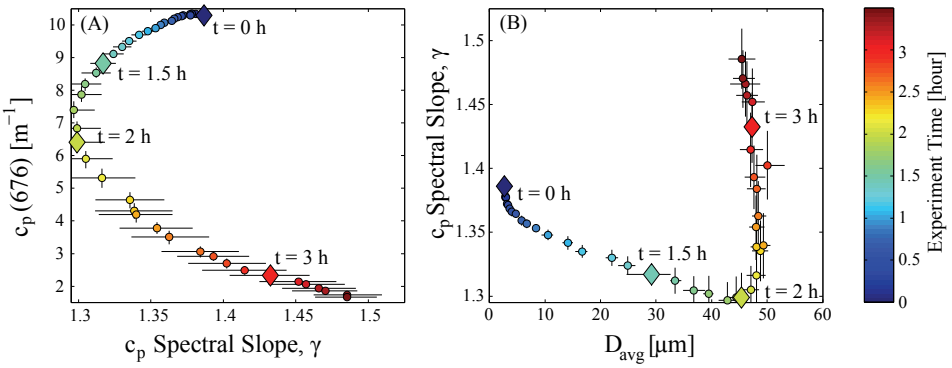

Fig. 8. – (A) Relationship between beam-attenuation magnitude and slope over the course of the laboratory experiment. (B) Relationship between spectral slope and average particle size. Diamonds signify data points corresponding to the experiment times identified in the figure.

4. Summary

The *in situ* and laboratory experiments described here suggest a greater role for aggregation and disaggregation in interpretation of optical properties and their variability than previously assumed. The *in situ* disaggregation experiment suggests large differences in beam-attenuation for the same mass with different packaging. This result also implies that the disturbance of samples due to pumping could introduce a bias in currently-employed field protocols, where turbulent shear from flow within an instrument or due to a sampling platform or vehicle could affect observations by breaking aggregates.

The settling experiment suggests that aggregates are much more efficient scatterers per mass that previously expected based on Mie theory for single particles. As aggregates formed and then sank, the relationship between optical properties and mass remained remarkably constant, consistent with previous work based on Latimer's model of attenuation by aggregates [14–16]. In addition, results from the aggregation-settling experiment support relationships between beam-attenuation magnitude and spectral slope as indicators of particle dynamics that have been observed in the field.

Other optical parameters we found to be sensitive to aggregation were (1) the ratio of beam-attenuation and total particulate volume as measured by the LISST, which is indicative

#141939 - $15.00 USD Received 28 Jan 2011; revised 22 Mar 2011; accepted 31 Mar 2011; published 11 Apr 2011

of packaging (and/or size) parameter in both experiments, and (2) the ratio of the beam-attenuation of ac-9 to that of the LISST, indicative of proportional increase in particles larger than 20 μm, due to the different acceptance angles of the two instruments. For aggregating particles, we did not find in our lab experiment that the information from spectral measurements of the VSF in the back direction provided as clear a picture of changes in particle size as that of spectral particulate beam-attenuation. More work is needed to understand the spectral shape of backscattering for natural particles.

In all but the simplest environments, attempting to understand how particle dynamic processes such as settling and aggregation affect observed optical properties is difficult, as examining hypotheses is muddied due to the presence of other ongoing processes, such as advection or local resuspension. The results presented here reinforce the use of *in situ* manipulation and idealized lab experiments where processes can be studied in isolation, as frameworks to help interpret field observations. Indeed, while we think these experiments are useful in isolating the effects of individual processes on optical properties, it is important to recognize their limitations as well. In this work, our measurements have focused on sediment-dominated systems, first near-bottom in an estuary, and second laboratory clays aggregated in salt. We expect that many of our results will be widely applicable, but must also acknowledge that in other cases such as large highly-absorbing phytoplankton aggregates, our understanding is incomplete and additional research is needed.

Acknowledgements

This work has been funded by the Environmental Optics Program of the Office of Naval Research (contract N00014-10-1-0508). The authors are grateful for the many interesting discussions of aggregates and optics with Tim Milligan (Bedford Institute of Oceanography) and Dr. Paul Hill (Dalhousie University). Special thanks to James Loftin (University of Maine) for assistance with the laboratory and field experiments. Thanks also to Dr. Yogi Agrawal (Sequoia Scientific) for providing one of the LISST-100 instruments for the field experiment, as well as Dr. Ivona Cetinić and Dr. Burt Jones (University of Southern California) for providing the ECO-BB3 used in the laboratory experiment. Thoughtful comments from two reviewers helped us improve upon our submitted manuscript.

#141939 - $15.00 USD Received 28 Jan 2011; revised 22 Mar 2011; accepted 31 Mar 2011; published 11 Apr 2011